

Preliminary Spectral Analysis of SN 1994I

E. Baron¹, P. H. Hauschildt², D. Branch¹, R. P. Kirshner³, and A. V. Filippenko⁴

¹*Dept. of Physics and Astronomy, University of Oklahoma, 440 W. Brooks, Rm 131, Norman, OK 73019-0225.*

²*Dept. of Physics and Astronomy, Arizona State University, Tempe, AZ 85287-1504.*

³*CfA, 60 Garden Street, Cambridge, MA 02138.*

⁴*Dept. of Astronomy, University of California, Berkeley, CA 94720-3411.*

21 March 2018

ABSTRACT

We present optical spectra of the Type Ic supernova 1994I in M51 and preliminary non-LTE analysis of the spectra. Our models are not inconsistent with the explosions of C+O cores of massive stars. While we find no direct evidence for helium in the optical spectra, our models cannot rule out small amounts of helium. More than $0.1 M_{\odot}$ of helium seems unlikely.

Key words: stars: evolution — supernovae: general — supernovae: individual (SN 1994I).

1 INTRODUCTION

The last few years have produced well observed supernovae of nearly every subclass. Of all the subclasses, the progenitors of Type Ib/c supernovae are the least well understood. Type I supernovae are classified by the lack of strong Balmer lines in their spectra. Whereas Type Ia supernovae are characterized by strong Si II lines and Type Ib supernovae by prominent He I lines, in Type Ic supernovae these features are weak or absent altogether. Supernova 1994I in M51 has been classified as a SN Ic (Phillips, 1994; Clocchiatti et al., 1994). While there is little doubt that SNe Ia are the result of the complete disruption of a white dwarf, several models have been proposed for the progenitors of Type Ib and Type Ic supernovae. The prominence of He I lines in Type Ib supernovae suggests that these SNe are due to the collapse of the helium core of a massive star, whose hydrogen envelope has been lost in a wind, or through a binary interaction. However, such a model fails to fit the long time behavior of the light curve of SN 1984L (Baron, Young, & Branch, 1993). Several groups have suggested that the progenitors of SNe Ic are due to collapse of C+O cores of massive stars, where both the hydrogen and helium envelopes have been stripped in either a Wolf-Rayet phase, or via binary interaction (Wheeler & Harkness, 1990; Filippenko, Porter, & Sargent, 1990; Podsiadlowski, Joss, & Hsu, 1992; Woosley, Langer, & Weaver, 1993; Nomoto et al., 1994). Based on the very early light curve of SN 1994I, Nomoto et al. (1994) have proposed that single star Wolf-Rayet models are ruled out and have described several possible evolutionary paths for the progenitor of SN 1994I. Further modeling of the light curve has suggested a very low mass for the ejecta, $M_{\text{ejecta}} \approx 0.9 - 1.4 M_{\odot}$ (Iwamoto et al., 1994; Woosley, Langer, & Weaver, 1995; Young, Baron, & Branch, 1995).

2 SPECTRAL MODELS

In order to provide model constraints the observed spectra must be modeled in detail. We use the generalized stellar atmosphere code PHOENIX 4.8 to compute model atmospheres and synthetic spectra for SN 1994I. This is an updated version of the code used for the analysis of the early spectra of Nova Cygni 1992 (Hauschildt et al., 1994), described there, in Allard et al. (1994), in Hauschildt et al. (1995), in Baron, Hauschildt, & Branch (1994), and in Baron et al. (1995). Thus, here we only briefly outline the calculational methods.

PHOENIX uses an accelerated Λ -iteration (ALI or operator splitting) method to solve the time independent, spherically symmetric, *fully* relativistic radiative transfer equation for lines and continua, to all orders in v/c including the effects of relativistic Doppler shift, advection, and aberration (Hauschildt, 1992a). The multi-level, non-LTE rate equations are solved self-consistently using an ALI method (Rybicki & Hummer, 1991; Hauschildt, 1993). Models atoms for H I, He I, He II, Mg II, Ca II, Na I, and Ne I have been implemented. Simultaneously we solve for the special relativistic condition of radiative equilibrium in the Lagrangian frame (Hauschildt, 1992b) using either a partial linearization or a modified Unsöld-Lucy temperature correction scheme. The relativistic effects, in particular the first order effects of advection and aberration, are important at the high expansion velocities observed in typical SNe (Hauschildt, Best, & Wehrse, 1991).

In addition to the non-LTE lines, the models include, self-consistently, line blanketing of the most important ($\approx 10^5$) metal lines selected from the latest atomic and ionic line list of Kurucz (1993). The entire list contains close to 42 million lines, but not all of them are important for the case at hand; the lines are dynamically selected according

to whether the ratio $\Gamma \equiv \kappa_l/\kappa_c$ is larger than a pre-specified value (usually 10^{-3}), where κ_l , κ_c are the absorption coefficients in the line center, and in the corresponding (LTE + non-LTE) continuum, respectively. In the subsequent radiative transfer calculations all lines selected in this way are taken into account as individual lines by opacity sampling, and all others from the large line list are neglected. We treat line scattering in the metal lines by parameterizing the albedo for single scattering, α . The calculation of α would require a full non-LTE treatment of *all* lines and continua, which is outside of the scope of this paper. Tests have shown that as a direct result of the velocity gradient in nova and supernova photospheres, the shape of the lines does not depend sensitively on α and our approach is a reasonable first approximation. Therefore, we adopt a constant value of $\alpha = 0.95$ for all metal lines. The continuous absorption and scattering coefficients are calculated using the cross-sections as described in Hauschildt et al. (1992).

The effects of non-thermal collisional ionization by primary electrons produced by collisions with gamma rays due to the decay of ^{56}Ni and ^{56}Co are modeled using the continuous slowing down approximation (Garvey & Green, 1976; Swartz, 1991). We have also included ionizations due to secondary electrons (Swartz, 1991), but most of their energy is thermalized and therefore has only a small effect on the level populations (Meyerott, 1980). The collisional cross sections are taken from the work of Lotz (1967a,b, 1968a,b,c).

The model atmospheres are characterized by the following parameters (see Hauschildt et al., 1992; Baron et al., 1995, for details): (i) the reference radius R_0 , which is the radius where the continuum optical depth in extinction at 5000 \AA (τ_{std}) is unity, (ii) the effective temperature T_{eff} , which is defined by means of the luminosity, L , and the reference radius, R_0 , ($T_{\text{eff}} = (L/4\pi R_0^2\sigma)^{1/4}$ where σ is Stefan’s constant), (iii) the density structure parameter, v_e , ($\rho(r) \propto \exp(-v/v_e)$), or N ($\rho(r) \propto (v/v_0)^{-N}$), (iv) the expansion velocity, v_0 , at the reference radius, (v) the density, ρ_{out} , at the outer edge of the envelope, (vi) the albedo for line scattering (metal lines only, here set to 0.95), (vii) the statistical velocity ξ , treated as depth-independent isotropic turbulence and set to 50 km s^{-1} for the models presented here, and (viii) the element abundances.

In order to minimize the parameters in setting the element abundances we begin with a solar abundance (Anders & Grevesse, 1989), and then “burn” hydrogen to helium with a final number ratio given by $[\text{He}/\text{H}] = \log_{10}(n_{\text{He}}/n_{\text{H}})$. Next we “burn” helium to carbon and oxygen with a final number ratio He/O , and a production ratio (by number) of carbon to oxygen C/O . Finally we allow metals heavier than oxygen to be scaled by the factor z . Thus, our abundance parameters consist of $[\text{He}/\text{H}]$, He/O , C/O , and z . In order to further reduce the size of parameter space we have used the results from the models of Iwamoto et al. (1994) and Woosley, Langer, & Weaver (1995) as guidance to fix the parameter $\text{C}/\text{O} = 0.5$. The mass fractions for the models presented are listed in Table 1.

For convenience, we have assumed an explosion date of March 30, 1994 to scale the radii of our models. We have confirmed that changes of a few days in the explosion date have very small effects on the shape of the output spectrum although the absolute flux obviously scales with the square of the radius, which we account for. We adopt an extinction

Table 1. Abundances of Presented Models

Model	X_{He}	X_{C}	X_{O}
April 3, low helium	0.05	0.25	0.68
April 3, high helium	0.35	0.17	0.46
April 11	1.8×10^{-4}	0.27	0.71
April 18	1.8×10^{-4}	0.27	0.71

The mass fractions of helium, carbon, and oxygen used in the models.

to the supernova of $E(B - V) = 0.45 \text{ mag}$, which we discuss further in §4. In order to avoid calculational difficulties, we have treated He II in LTE.

Since our models do not include NLTE treatments of all the relevant ions (in particular O I, O II, C I, C II, Si II, and Fe II are treated in LTE), we cannot, as yet, provide quantitative abundance estimates. We can, however, draw qualitative conclusions based on our modeling. In future work we will present calculations including a ≈ 617 level Fe II model atom (Hauschildt & Baron, 1995).

While we only present results of our “best fits” (as determined by eye, comparing to the complete observed spectrum) we have in fact calculated more than 100 models, where we have varied the He abundance by factors of 10,000, we have examined models from 1/2 solar to 6 times solar metallicity, and we have varied the C/O production ratio by a factor of 3. All of the models discussed in this paper are available upon request.

3 SPECTRA AND RESULTS

Figure 1 displays the data obtained on April 3.5, 1994 UT at the MMT as well as our calculated model with $T_{\text{eff}} = 8300 \text{ K}$, $v_0 = 12000 \text{ km s}^{-1}$, $N = 6$, $X_{\text{Ni}} = 0.01$, $[\text{He}/\text{H}] = 12$, $\text{He}/\text{O} = 0.3$, $\text{C}/\text{O} = 0.5$, and $z = 3$. Our boundary conditions were for the outer radius and density were $R_{\text{out}} = 1.96 \times 10^{15} \text{ cm}$ and $\rho_{\text{out}} = 3.93 \times 10^{-17} \text{ g cm}^{-3}$. The line identifications correspond to the results of our theoretical models and we try to indicate where model limitations may be inaccurate. The synthetic spectrum is dominated by Ca II and C II lines, although Fe II and O II lines are also present. The synthetic spectrum fits the Ca II H+K emission profile very well, but the emission near 4500 \AA is too weak. It fits the broad absorption feature near 5000 \AA reasonably well, but there is too little absorption and the emission is too strong. In our model spectrum the emission is due to Fe II and Mg I lines. It is likely that NLTE treatments of S II, Si II and C II would better reproduce the observed spectrum. Also plotted in Figure 1 is the synthetic spectrum for a model with $N = 8$, giving a steeper atmosphere. The other parameters were the same but in order to better reproduce the observed spectrum $v_0 = 15000 \text{ km s}^{-1}$. The lines are too narrow in the steeper model in spite of the fact that the velocity is larger. As to be expected, the steeper model only enhances the mismatch with the observed spectrum in the red since the Fe II and C II lines become more pronounced. There is no clear evidence of He I lines in our synthetic spectrum and reducing the helium abundance by a factor of 10 does not significantly affect the spectrum. Increasing the helium abundance by a factor of 10 still fails to show clear evidence for He I lines, but the quality of the overall fit is signif-

icantly reduced, (see Figure 1); the Ca II H+K emission becomes too broad, and the feature near 4500 Å becomes very flat in absorption with only weak emission. Thus, at present, we can not easily determine the amount of helium in the ejecta. Higher amounts of helium do begin to show the effects of He I. In the model with high helium abundance (He/O= 3.0), the helium mass fraction is $Y = 0.35$ and the total mass above the $\tau_{\text{std}} = 1$ (30) is 0.08 (0.34) M_{\odot} , respectively. For the model with He/O= 0.3, the helium mass fraction is $Y = 0.05$. Near-IR spectra including the He I $\lambda 10830$ line would be extremely useful for determining the helium abundance.

We display in Figure 2 the observed spectrum for April 11.5, 1994 UT obtained at the MMT along with our best fit synthetic spectrum. The model parameters are: $T_{\text{eff}} = 6650$ K, $v_0 = 8000$ km s $^{-1}$, $N = 8$, $X_{\text{Ni}} = 0.02$, [He/H]= 12, He/O= 0.001, C/O= 0.5, $z = 4$, $R_{\text{out}} = 2.13 \times 10^{15}$ cm, and $\rho_{\text{out}} = 5.04 \times 10^{-17}$ g cm $^{-3}$. The observed spectrum now displays lines of S II, Si II, Na I, and O I, in addition to Ca II and Fe II lines. The O I $\lambda 7773$ line is clearly evident (and not too badly fit). The calculated Ca II H+K red absorption edge does not quite extend far enough to the blue although the width of emission profile is about right. The S II absorption to the red of 5000 Å is not broad enough. The observed absorption feature near 5600 Å, almost certainly due to Na I, is poorly fit. Also poorly fit is the observed absorption near 6200Å, likely due to Si II $\lambda 6355$. A NLTE treatment of Si II and S II would likely improve the agreement between theory and observation. The high metallicity is required in order to obtain good agreement with the spectra, and is consistent with the position of the supernova close to the nucleus and observational determinations of the metallicity of M51 (Diaz et al., 1991).

The observed spectrum obtained on April 18, 1994 at Lick Observatory is displayed in Figure 3, along with our best fit synthetic spectrum with model parameters: $T_{\text{eff}} = 5300$ K, $v_0 = 8000$ km s $^{-1}$, $N = 8$, $X_{\text{Ni}} = 0.01$, [He/H]= 13, He/O= 0.001, C/O= 0.5, $z = 4$, $R_{\text{out}} = 3.9 \times 10^{15}$ cm, and $\rho_{\text{out}} = 6.4 \times 10^{-17}$ g cm $^{-3}$. The C I $\lambda 9088$ and $\lambda 9641$ lines are clearly identified as is the O I $\lambda 7773$ line, even if the agreement with observations is poorer than desired. At this time, the calcium profiles for the H+K lines and the IR triplet are sensitive to the amount of ^{56}Ni as well as to the density profile. More nickel leads to narrower profiles since it ionizes calcium at high velocity. The red edge of the calcium IR triplet absorption profile is a bit too fast which may be due to the density profile deviating from our assumed power-law. The red edge of the calcium IR triplet can be better fit and the large emission in the infrared triplet can be suppressed by making the atmosphere shallower, but then the overall fit to the rest of the observed spectrum is significantly degraded. We also find that better fits to the calcium profile can be obtained with a lower velocity $v_0 = 7000$ km s $^{-1}$, but this leads to large emission in the 4000–6000 Å range that no choice of temperature can improve, as well as a much poorer fit to the O I absorption.

4 REDDENING

The strong interstellar sodium line visible in all observed spectra is evidence for a significant amount of reddening in

SN 1994I; The observed position of the supernova coincides with a dust finger in the host galaxy M51. Based on an overall fit to the light curve Iwamoto et al. (1995) find an extinction of $A_V = 1.4$ mag, while an analysis of the Na D absorption finds $A_V = 3.1^{+3.1}_{-1.5}$ mag (Ho & Filippenko, 1995). One can use the earliest spectrum on April 3 to estimate the reddening. The observed spectrum displays strong absorption in Ca II H+K. However, as the reddening increases, the color temperature of the synthetic continuum spectrum must also increase in order to match the observed spectrum. But this higher temperature depopulates the lower level of the Ca H+K lines and hence the strong absorption seen in the spectrum cannot be reproduced. Figure 4 displays our calculated spectra for $T_{\text{eff}} = 8300, 8600,$ and 9100 K. We find that the temperature is fairly well determined $T_{\text{eff}} \approx 8300$ K, although it may be possible to go to higher temperatures by confining calcium to cooler regions. On the other hand, our models produce reasonably good agreement with the red edge of the calcium absorption which indicates that we do not have calcium mixed too deeply. Using the reddening law of Cardelli, Clayton, & Mathis (1989) we find that extinctions $0.9 \lesssim A_V \lesssim 1.4$ mag provide good fits to the observed spectrum at this epoch, and that $A_V \approx 1.4$ mag is clearly favored at later epochs.

5 DISCUSSION AND CONCLUSIONS

The nickel abundance is not well determined by our models due to the fact that our deposition function is local, and even at maximum light not all of the gamma rays are trapped with such low mass ejecta. Our results are consistent with the small nickel masses implied by light curve analyses.

Wheeler et al. (1995) have identified the absorption feature near 6200 Å as being due to Si II $\lambda 6355$. Although in all of our models the absorption near 6200 Å is due to C II and Ba II, the fit to observations is poor. In order to correctly fit the observed spectrum, it is likely that Si II needs to be treated in NLTE. It is not surprising that our results are different from those of Wheeler et al. (1995); even though both calculations treat Si II in LTE, our self-consistent temperature structure is likely to differ from the grey temperature structure of Wheeler et al. (1995).

The uncertain rise-time and reddening of SN 1994I make it a less than ideal candidate for the spectral-fitting expanding atmosphere method (SEAM, see Baron et al., 1995; Nugent et al., 1995); note that we have corrected an error in our synthetic photometry that was present in those papers]. Nevertheless, the absolute flux is a direct result of our models, and the predicted distances serve as a useful check on the accuracy of the synthetic spectra. Applying this method to SN 1994I, with an assumed reddening of $E(B - V) = 0.45$ mag, we find a bolometric rise-time of 9 days, and a distance modulus to the supernova of $\mu = 28.9 + 5 \log(t_r/9 \text{ days}) \pm 0.5 \pm 0.7$ mag, where the first uncertainty is simply the standard deviation in all our fits and the second uncertainty is an estimate of our systematic error (Nugent et al., 1995) including an estimate of the error due to the uncertain reddening correction. In principle, the distance estimate gives a value for the rise-time, by minimizing the scatter in distance obtained at different epochs, but for SN 1994I the uncertain reddening, and the use of only 3

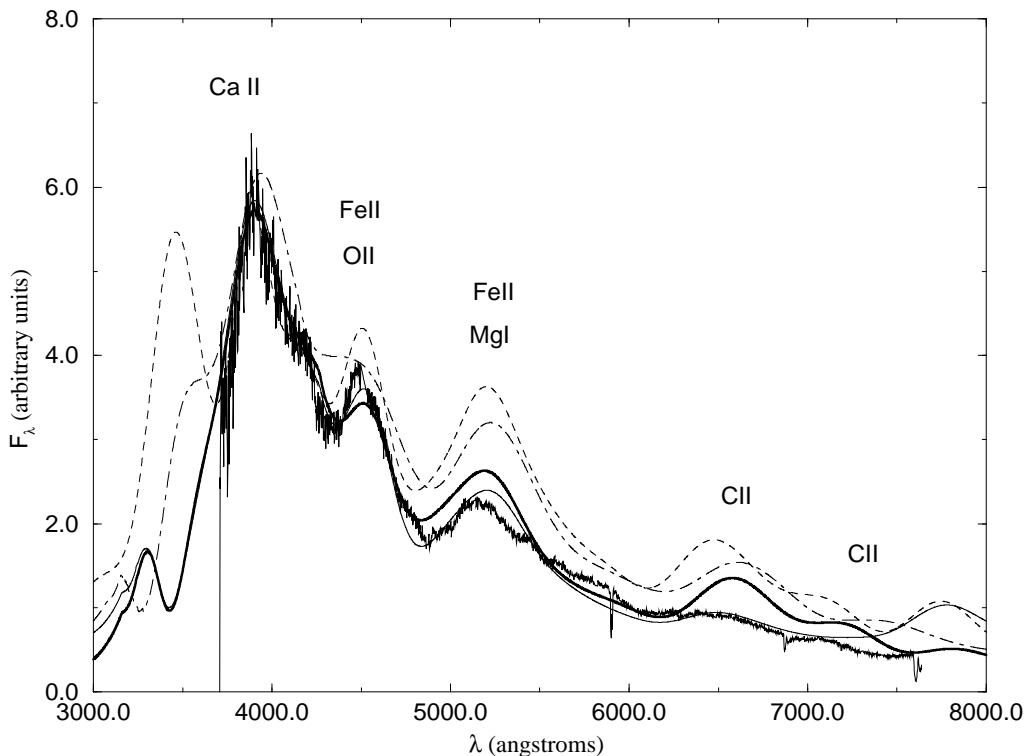


Figure 1.

Observed and synthetic spectra for April 3, 1994. The observed spectrum has been dereddened with $E(B-V) = 0.45$ mag. The absorption features near 6860 \AA and 7600 \AA are telluric. For the calculated models the parameters are $T_{\text{eff}} = 8300 \text{ K}$, $v_0 = 12000 \text{ km s}^{-1}$, $N = 6$, $X_{\text{Ni}} = 0.01$, $[\text{He}/\text{H}] = 12$, $\text{He}/\text{O} = 0.3$, $\text{C}/\text{O} = 0.5$, and $z = 3$ (thick solid line), the same parameters but $\text{He}/\text{O} = 3.0$ (dot-dashed line) and the same parameters but $N = 8$, $v_0 = 15000 \text{ km s}^{-1}$, and $\text{He}/\text{O} = 0.3$ (dashed line). The thin solid line corresponds to a model with the same parameters as the thick solid line, but C II lines have been removed from the line-list in the theoretical spectrum.

epochs with one before maximum light, makes such a determination ambiguous. The rise-time should be compared to the results of Iwamoto et al. (1994), who find a 12 day rise-time for models of the light-curve of SN 1994I.

Comparing our results to published hydrodynamical models of the light curve of SN 1994I, we find that our models have substantial mass above the reference radius. On April 18, the mass above the reference radius ranges from $0.5 M_{\odot}$ for our shallowest models to $1.6 M_{\odot}$ for our steepest models. The steeper, more massive model produces a significantly better fit to the observed spectrum than the shallower, less massive model, but since the Ca II profile is sensitive to the density profile and given our simplifying assumptions of uniform compositions and a power law density profile it would be premature to draw conclusions about the density structure from our models.

Although the two published hydrodynamical models of the light curve of SN 1994I are from very different stellar evolution scenarios (Woosley, Langer, & Weaver, 1995; Iwamoto et al., 1994), the actual models are very similar in total ejected mass, total nickel mass, and energy of explosion. Without performing detailed synthetic spectral

modeling of each calculation it is difficult for us to favor one stellar evolution scenario or the other.

Our calculations lend credence to the identification of SNe Ic progenitors as C+O cores formed in an interacting binary (Wheeler & Harkness, 1990). In order to make definitive statements about abundances, more intermediate mass elements need to be included in NLTE. Additionally, non-uniform compositions need to be treated. However, once the atmospheres become inhomogeneous, parameter space becomes larger than can be adequately covered. A better way to proceed is to perform spectroscopic diagnostics on hydrodynamical models. In order to do this in an objective manner, hydrodynamical calculations must fully resolve the density profile in the atmosphere.

ACKNOWLEDGMENTS

We are most grateful to Brian Schmidt for providing the MMT spectra quickly and for helpful comments on the manuscript. We thank Adam Fisher and Sumner Starrfield for helpful discussions, and Ken Nomoto for providing us

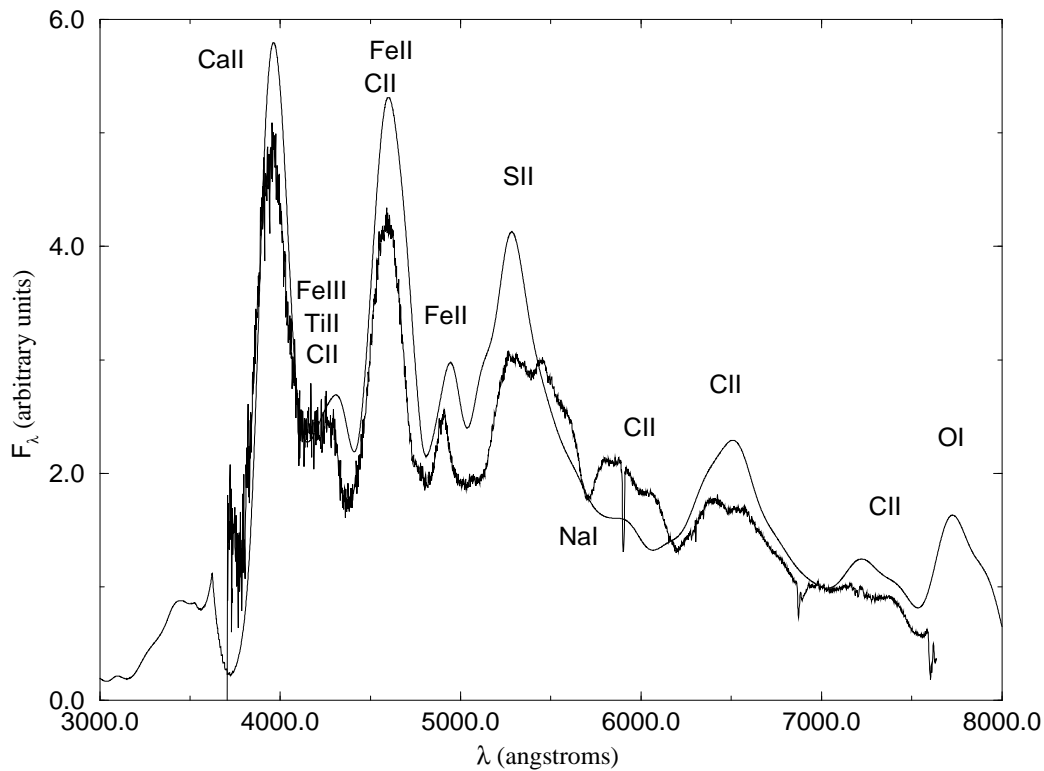


Figure 2.

Observed and synthetic spectra for April 11.5, 1994. The observed spectrum has been dereddened with $E(B-V) = 0.45$ mag. The absorption features near 6860 Å and 7600 Å are telluric.

with the results of his hydro models. Assistance with the observations and reductions at Lick Observatory was provided by Luis C. Ho and Aaron J. Barth. This work was supported in part by NASA grant NAGW-2999, a NASA LTSA grant to ASU, NASA grant GO-2563.01-87A from the Space Telescope Science Institute, which is operated by the Association of Universities for Research in Astronomy, Inc., and by NSF grants AST-9115061 and AST-9115174. Some of the calculations in this paper were performed at the NERSC, supported by the U.S. DoE, and at the San Diego Supercomputer Center, supported by the NSF; we thank them for a generous allocation of computer time.

REFERENCES

- Allard, F., Hauschildt, P. H., Miller, S., & Tennyson, J. 1994, *ApJ (Letters)*, 426, L39
- Anders, E., & Grevesse, N. 1989, *Geochim. Cosmochim. Acta*, 53, 197
- Baron, E., Young, T., & Branch, D. 1993, *ApJ*, 409, 471
- Baron, E., Hauschildt, P. H., & Branch, D. 1994, *ApJ*, 426, 334
- Baron, E., Hauschildt, P. H., Branch, D., Austin, S., Garnavich, P., Ann, H. B., Wagner, R. M., Filippenko, A. V., Matheson, T., & Liebert, J. 1995, *ApJ*, 441, 170
- Cardelli, J. A., Clayton, G. C., & Mathis, J. S. 1989, *ApJ*, 345, 245
- Clocchiatti, A., Brotherton, M., Harkness, R. P., & Wheeler, J. C. 1994, *IAU Circ.*, No. 5972
- Diaz, A. I., Terlevich, E., Vilchez, J., Pagel, B., & Edmunds, M. G. 1991, *MNRAS*, 253, 245
- Filippenko, A. V., Porter, A. C., & Sargent, W. L. W. 1990, *AJ*, 100, 1575
- Garvey, R. H., & Green, A. E. S. 1976, *Phys. Rev. A*, 14, 946
- Hauschildt, P. H. 1992a, *JQSRT*, 47, 433
- Hauschildt, P. H. 1992b, *ApJ*, 398, 224
- Hauschildt, P. H. 1993, *JQSRT*, 50, 301
- Hauschildt, P. H., & Baron, E. 1995, *JQSRT*, in press
- Hauschildt, P. H., Best, M., & Wehrse, R. 1991, *A&A*, 247, L21
- Hauschildt, P. H., Wehrse, R., Starrfield, S., & Shaviv, G. 1992, *ApJ*, 393, 307
- Hauschildt, P. H., Starrfield, S., Austin, S., Wagner, R. M., Shore, S. N., & Sonneborn, G. 1994, *ApJ*, 422, 831
- Hauschildt, P. H., Starrfield, S., Shore, S. N., Allard, F., & Baron, E. 1995, *ApJ*, 447, 829
- Ho, L. C., & Filippenko, A. V. 1995, *ApJ*, 444, 165
- Iwamoto, K., Nomoto, K., Höflich, P., Yamaoka, H., Kumagai, S., & Shigeyama, T. 1994, *ApJ (Letters)*, 437, L115

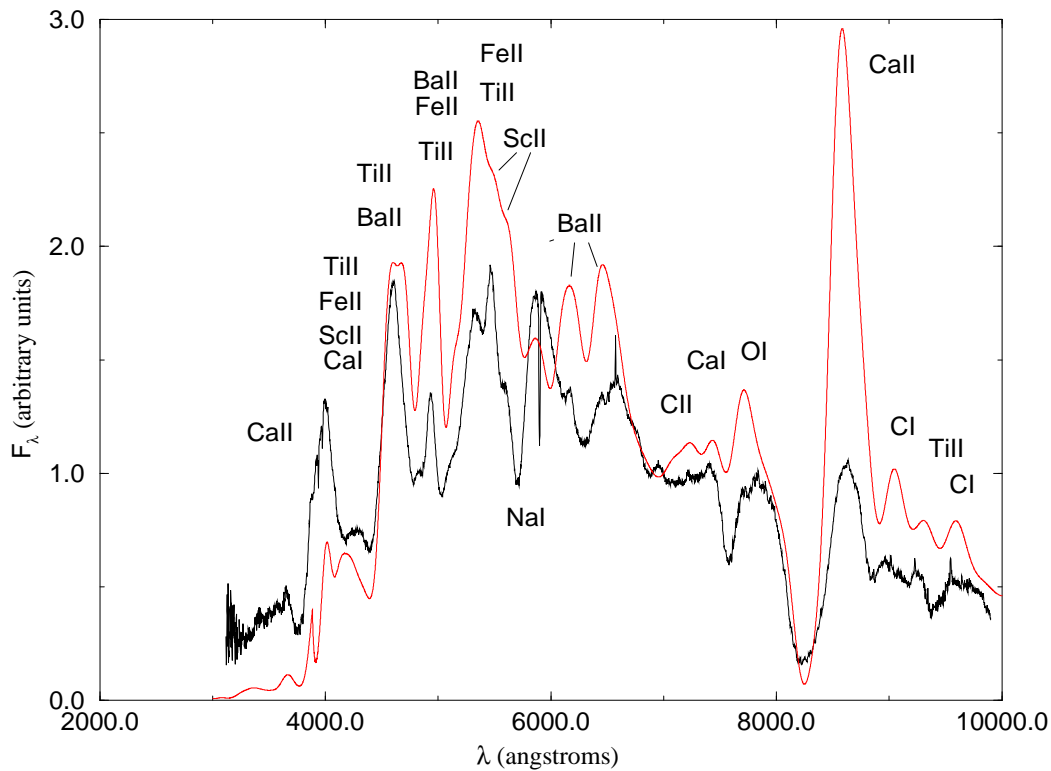


Figure 3.

Observed and synthetic spectra for April 18, 1994. The observed spectrum has been dereddened with $E(B-V) = 0.45$ mag. All telluric features have been removed.

Kurucz, R. 1993, CDROM No. 1 Atomic Data for Opacity Calculations, SAO Cambridge, MA

Lotz, W. 1967a, ApJ Suppl., 14, 207

Lotz, W. 1967b, Journal Opt. Soc. America, 57, 873

Lotz, W. 1968a, Journal Opt. Soc. America, 58, 236

Lotz, W. 1968b, Journal Opt. Soc. America, 58, 915

Lotz, W. 1968c, Z. Physik, 216, 241

Meyerott, R. E. 1980, ApJ, 239, 257

Nomoto, K., Yamaoka, H., Pols, O. R., van den Heuvel, E. P. J., Iwamoto, K., & Shigeyama, T. 1994, Nature, 371, 227

Nugent, P., Baron, E., Hauschildt, P., & Branch, D. 1995, ApJ (Letters), 441, L33

Phillips, M. M. 1994, IAU Circ., No. 5966

Podsiadlowski, P., Joss, P. C., & Hsu, J. J. L. 1992, ApJ, 391, 245

Rybicki, G. B., & Hummer, D. G. 1991, A&A, 245, 171

Swartz, D. 1991, ApJ, 373, 604

Wheeler, J. C., & Harkness, R. 1990, Repts. Prog. Phys., 53, 1467

Wheeler, J. C., Harkness, R. P., Clocchiatti, A., Benetti, S., Brotherton, M. S., DePoy, D. L., & Elias, J. 1995, ApJ (Letters), 436, L135

Woosley, S. E., Langer, N., & Weaver, T. A. 1993, ApJ, 411, 823

Woosley, S. E., Langer, N., & Weaver, T. A. 1995, ApJ, 448, 315

Young, T. R., Baron, E., & Branch, D. 1995, ApJ (Letters), 449, L51

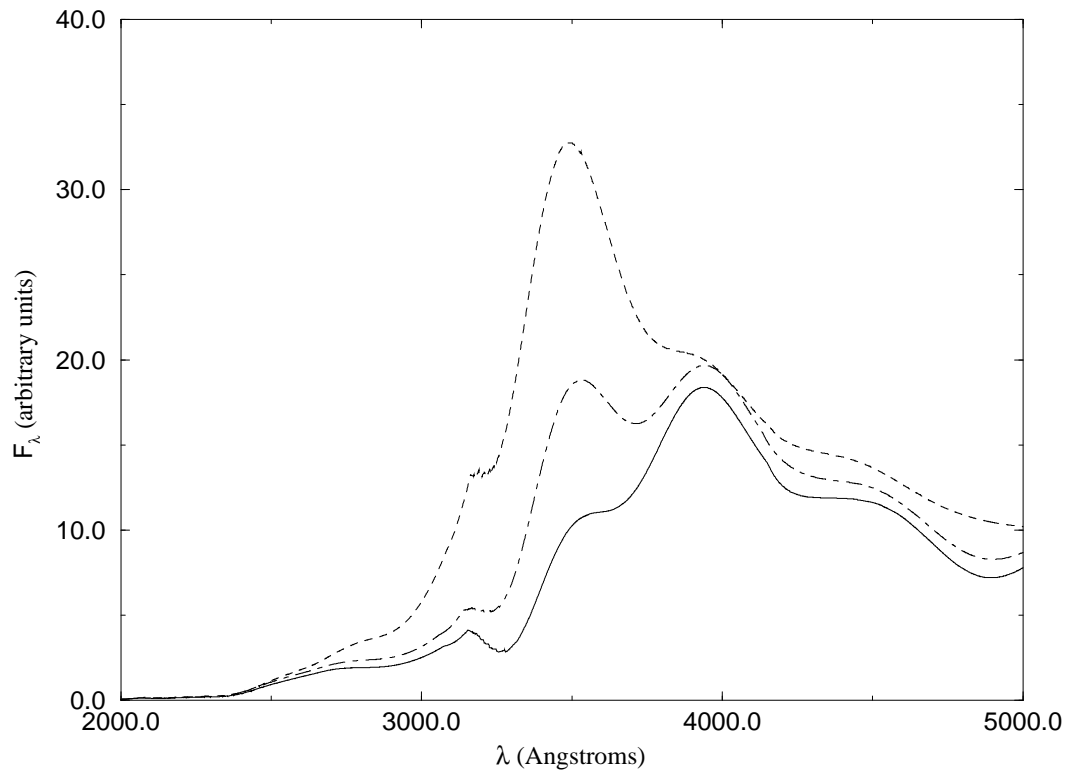


Figure 4.

Synthetic spectra with $T_{\text{eff}} = 8300$ (solid line), 8600 (dot-dashed line), and 9100 K (dashed line).